Tuned Sloshing Dampers in Tall Buildings Considering Floor Tilt

J. S. Love, M.ASCE[1]; and K. P. McNamara[2]

Abstract: Tuned sloshing dampers (TSDs) are used to reduce the wind-induced motion of tall buildings to improve occupant comfort. Tall, slender structures experience dynamic tilt as they deflect in bending; however, this tilting is typically ignored when designing a TSD system and has not received attention in the literature. Two models—a nonlinear multimodal model and a linearized equivalent mechanical model—are developed to accommodate the effects of tilting on the sloshing response and structure–TSD interaction. Tower tilt causes a component of gravitational acceleration to increase the effective lateral acceleration felt by the TSD tank, which increases the TSD excitation and response. Conversely, the second time derivative of tower tilt serves to decrease the TSD excitation; however, this term is generally small for most TSDs. Overall, tower tilt increases the effective mass of the TSD, which improves the efficacy of the device for a given TSD tank size. The sloshing response, including wave heights and TSD base shear forces, is increased because of the tower tilt, and it is therefore unconservative to ignore this effect when establishing tank design loads. A case study is presented wherein a real-world tower is equipped with a TSD and the influence of tilt is studied. For this tower, the effective mass of the TSD is increased by a factor of 1.1 due to the tower tilt, which enabled the width of the tank to be decreased by a factor of 1.1 while maintaining the same performance. Including tower tilt enables smaller TSD tanks to be employed, saving valuable real estate at the top of tall buildings. With current prices per square meter of usable floor area at the top of a luxury tall building, it is estimated that the space savings would be valued at hundreds of thousands of dollars. **DOI: 10.1061/JSDCCC.SCENG-2077.**

Author keywords: Tuned sloshing dampers (TSDs); Tall building tilt; Equivalent mechanical model; Nonlinear multimodal sloshing model; Structural control.

Introduction

Over the last several decades, there has been a trend to build taller and more slender structures around the world, particularly across North America, Australia, the Middle East, India, and China. Modern construction materials and design techniques have enabled these structures to withstand the large gravity and lateral loads to which they are subjected while minimizing the use of construction materials. As a result, these buildings are lightweight, flexible, and generally possess very low inherent damping, which has led to the potential for significant wind-induced motion that negatively affects serviceability limit states. Large tower motions lead to occupant comfort complaints arising from annoying felt motions, elevator malfunction, and noises from squeaking partitions (Griffis 1993; Irwin et al. 2019; Kwok et al. 2015). Increasing the building's mass and stiffness will generally reduce motions; however, this is undesirable as this solution requires the use of more materials and reduces occupiable space as the structural member sizes increase. However, the very low damping inherent in these structures enables great opportunity for the implementation of supplementary damping systems.

[1]Technical Director, Motioneering Inc., 600 Southgate Dr., Guelph, ON, Canada N1G 4P6 (corresponding author). ORCID: https://orcid.org/0000-0003-2749-0241. Email: Shayne.Love@motioneering.ca

[2]Senior Engineer, Motioneering Inc., 600 Southgate Dr., Guelph, ON, Canada N1G 4P6. ORCID: https://orcid.org/0000-0002-6195-7725. Email: Kevin.McNamara@motioneering.ca

Note. This manuscript was submitted on May 9, 2025; approved on October 21, 2025; published online on June 19, 2026. Discussion period open until November 19, 2026; separate discussions must be submitted for individual papers. This paper is part of the ***Journal of Structural Design and Construction Practice***, © ASCE, ISSN 2996-5136.

The control of wind-induced motion of tall, slender buildings using tuned sloshing dampers (TSDs), also known as tuned liquid dampers (TLDs), has increased significantly in popularity over the last two decades. There are currently many dozens of tall buildings, either built or under construction, that employ a TSD system to reduce wind-induced motion (Love et al. 2021). A TSD is a tank that is partially filled with water and located near the top of the tower (Kareem and Sun 1987). When the building moves under a dynamic wind load, the water within the tank will begin to slosh. By selecting the proper tank dimensions, the natural sloshing frequency of the water is "tuned" to be close to the natural frequency of the tower, enabling the water to experience a substantial resonant response. Vibrational energy is thereby transferred from the moving structure to the sloshing water, where it is then dissipated by damping elements within the tank. Screens, baffles, or other flow obstructions are added to the tanks of modern TSDs to increase the liquid damping toward its optimal value (Tait 2008; Warnitchai and Pinkaew 1998).

Modeling sloshing water in a tank that is relatively shallow, with depth-to-length ratios generally ranging from 10% to 25%, can be difficult, since it is an inherently nonlinear phenomenon (Faltinsen and Timokha 2009). Moreover, the damping associated with liquid drag on the obstructions placed in the tanks is proportional to liquid velocity-squared, which produces nonlinear damping. At the conceptual design stage, when the TSD dimensions and performance are being initially estimated, it is common to employ statistical linearization (Caughey 1963) to model the sloshing fluid as an equivalent linearized mechanical model with amplitude-dependent damping (Tait 2008). An equivalent spring-mass-dashpot system is therefore developed, which requires iteration to solve, but can be readily implemented. This simplification disregards the nonlinear coupling that occurs among sloshing modes and is therefore often only appropriate at low levels of excitation associated with the most common wind events or deeper tanks. As the excitation amplitude grows, such as when design-level loading events are considered, it is necessary to employ nonlinear models that can accommodate the nonlinear coupling among sloshing modes. Nonlinear modal coupling can dramatically affect the response of the sloshing liquid, the design loads, and the performance of the system; therefore many different nonlinear models have been developed, including multimodal models (Faltinsen et al. 2000; Faltinsen and Timokha 2001), shallow-water wave theory (Lepelletier and Raichlen 1988; Tait et al. 2005), and smoothed particle hydrodynamics (McNamara et al. 2021; McNamara and Tait 2022). For all these nonlinear models, the tank is subjected to a base acceleration, and the resulting fluid response can be determined using time-domain analysis techniques. The sloshing forces generated by the TSD are then applied back onto the structure of the coupled structure–TSD systems at the next time step.

The wind-induced motion of tall buildings is composed of both shear racking and bending actions as shown schematically in Fig. 1. For shear racking actions, the floor slabs remain parallel to each other, and the deformation occurs due to shear in the lateral force resisting elements. For bending actions, the floor slabs rotate, as the deformation is produced by the exterior vertical load carrying elements (typically columns) elongating or compressing. In any building, the total deformation is composed of both actions; however, in tall, slender towers, bending becomes the dominant type of deformation (Smith and Coull 1991; Tamboli 2014); therefore the upper floors of these towers will tilt.

TSD models in the existing literature have generally assumed the liquid excitation arises solely from the lateral acceleration of the tank. However, for tall towers there will be some dynamic tilt (bending rotation) of the floor slab, which will also produce a sloshing response. To the authors' knowledge, no study has investigated how considering tower tilt will affect TSD performance and how it may enable more efficient TSDs or smaller TSD tank designs.

This study seeks to investigate the response and performance of TSDs when the tilt of a building's floor plate is considered. First, a nonlinear multimodal model is presented, which includes the effects of tilt and is solved using time-domain analysis. Subsequently, a linearized equivalent mechanical model is developed, which considers the effects of tilt on the structure–TSD interaction. The linearized equivalent mechanical model is solved using frequency-domain techniques. Using a real-world tower tested in the wind tunnel, the performance of a TSD system with and without the consideration of tilt is investigated. The results from the linearized equivalent mechanical model and the nonlinear multimodal model are compared to evaluate the two models and to demonstrate potential savings.

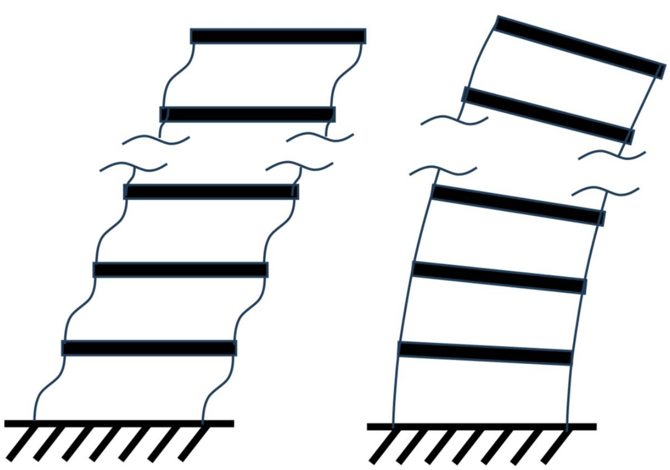

Fig. 1. Schematic (exaggerated) of shear racking deformation (left) and bending deformation (right) in a tall building.

Modeling

Although the tilting of slender, tall buildings is recognized, there are relatively little real-world tilt measurement data available. Tilt sensors have been used to monitor the very low-frequency (quasi-static) motion of structures due to thermal expansion (Pehlivan et al. 2015; Xia et al. 2014). Tilt sensors have also been used to perform modal identification (Zhang et al. 2019) and estimate tower deflection (Hu et al. 2020). For tall, slender structures whose deformation is dominated by bending, the tilt angle is equal to the derivative of the mode shape with respect to height (Hu et al. 2020)

$$\phi_\theta = \frac{\partial \phi_x}{\partial z} \tag{1}$$

The tower tilt may therefore be calculated from the modal information output by finite-element packages. Caution must be applied to buildings with nontrivial shear deformation; however, this is outside the scope of the current study. Lastly, it is assumed that the structural floor remains plane; that is, the floor slab does not bend in plane to produce different amounts of tilt across the floor plate.

The TSD tank is rectangular with a length, L, quiescent water depth, h, and width (into page), b, as shown in Fig. 2. The origin of the xz plane for the TSD is located at the free surface at the left end of the tank, and the y axis is pointing into the page. Flow obstructions are located a distance of x_{sc} from the tank end wall, and the flow obstructions have a loss coefficient of C_l. The tank is subjected to a base acceleration, $\ddot{X}$, and a tilt about the y axis, θ.

For both the multimodal model and equivalent mechanical model considered herein, the liquid is assumed to be inviscid, incompressible, and irrotational, which enables potential flow theory to be employed. In the following sections, a third-order nonlinear multimodal model is presented, followed by a linearized equivalent mechanical model. Both models require that the liquid response is dominated by the fundamental sloshing mode. For very shallow tanks experiencing large excitation amplitude, this assumption may not be realized as higher-order modes are easily excited nonlinearly; therefore, these models may not be appropriate in these cases.

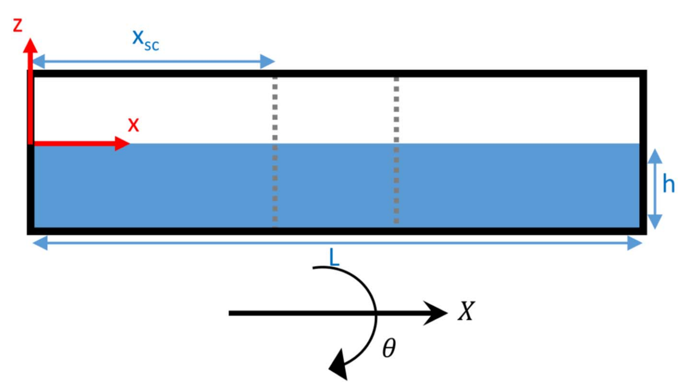

Fig. 2. Schematic of TSD tank under base motion with tilt.

Nonlinear Multimodal Model

An existing third-order nonlinear multimodal model is used to study the performance of a structure–TSD system with building tilt. The model accommodates the coupling among the first three sloshing modes and requires that the response of the fundamental sloshing mode is greater than the second sloshing mode, which in turn is greater than the third sloshing mode. While the original sloshing model could accommodate tank tilt (Faltinsen et al. 2000), the effects of tilt have not been considered for TSD applications. When tank tilt is included, the equations of motion for the TSD take the form (Faltinsen et al. 2000; Love and Tait 2010)

$$\begin{aligned}
&\ddot{\beta}_1 + 2\omega_1(\zeta_1^w + \zeta_1^{sc})\dot{\beta}_1 + \omega_1^2\beta_1 + d_1(\ddot{\beta}_1\beta_2 + \dot{\beta}_1\dot{\beta}_2) \\
&\quad + d_2(\ddot{\beta}_1\beta_1^2 + \dot{\beta}_1^2\beta_1) + d_3\ddot{\beta}_2\beta_1 + P_1(\ddot{X} - g\theta - S_1\ddot{\theta}) = 0 \\
&\ddot{\beta}_2 + 2\omega_2(\zeta_2^w + \zeta_2^{sc})\dot{\beta}_2 + \omega_2^2\beta_2 + d_4\ddot{\beta}_1\beta_1 + d_5\dot{\beta}_1^2 = 0 \\
&\ddot{\beta}_3 + 2\omega_3(\zeta_3^w + \zeta_3^{sc})\dot{\beta}_3 + \omega_3^2\beta_3 + d_6\ddot{\beta}_1\beta_2 + d_7\ddot{\beta}_1\beta_1^2 + d_8\ddot{\beta}_2\beta_1 \\
&\quad + d_9\dot{\beta}_1\dot{\beta}_2 + d_{10}\dot{\beta}_1^2\beta_1 + P_3(\ddot{X} - g\theta - S_3\ddot{\theta}) = 0
\end{aligned} \tag{2}$$

where β_i = generalized response of sloshing mode i; and the remaining damping terms, ζ_i^w and ζ_i^{sc}, coupling terms, d_i, and excitation terms, P_i and S_i, are based on the tank dimensions and are straightforward yet tedious to compute. For this reason, the interested reader is referred to their definitions and derivations elsewhere (Faltinsen et al. 2000; Love and Tait 2010). In Eq. (2), the excitation in Modes 1 and 3 includes a lateral acceleration term, $\ddot{X}$, as well as a tilt displacement, θ, and tilt acceleration, $\ddot{\theta}$ (second time derivative of tilt), term. The second mode is symmetric and is only excited through nonlinear coupling with Modes 1 and 3.

After the sloshing mode responses are determined at a time step using the Runge–Kutta–Gill method, the total lateral TSD force exerted on the structure is calculated as the summation of inertial components related to translation and tilt, as well as a sloshing component according to (Faltinsen and Timokha 2009)

$$F_{\mathrm{TSD}} = m_w\left(-\ddot{X} - g\theta - \frac{1}{2}h\ddot{\theta} + \frac{L}{\pi^2 h}\sum_{i=1}^{3}\ddot{\beta}_i\frac{1+(-1)^{i+1}}{i^2}\right) \tag{3}$$

Since the first three terms are proportional to the structural displacement and acceleration (translation and rotation), they function to add a small amount of stiffness and inertia/mass to the structure, but they do not dissipate energy. The final term is the most important term to the functioning of the TSD as it is proportional to the liquid sloshing response and dissipates energy when the TSD is well-tuned.

The wave heights at any location along the tank length are computed as (Faltinsen and Timokha 2009)

$$\eta(x,t) = \sum_{i=1}^{3}\beta_i\cos\left(\frac{i\pi}{L}x\right) \tag{4}$$

The structure is represented using modal analysis and has a generalized mass, damping constant, and stiffness of M, C, and K, respectively. The natural angular frequency and damping ratio of the structure are defined as $\omega_s = \sqrt{K/M}$ and $\zeta_s = C/2\mathrm{sqrt}(KM)$. The structure–TSD system is solved in the time domain by applying the external wind loading, F_{exc}, and TSD force, F_{TSD}, to the structure at each time step and solving the equation of motion of the structure

$$M\ddot{X} + C\dot{X} + KX = F_{\mathrm{exc}} + F_{\mathrm{TSD}} \tag{5}$$

Subsequently, the multimodal sloshing response is determined by solving Eq. (2), and the sloshing force to be applied to the structure at the next time step is determined using Eq. (3). In this study, the fourth-order Runge–Kutta–Gill method is used to solve this system of equations in the time domain. Scale model experiments of structure–TSD systems have shown that nonlinear multimodal models can accurately predict the response of these coupled systems (Love and Tait 2013).

Equivalent Mechanical Model

To develop the equivalent mechanical model, the procedure presented by (Tait 2008) is followed. However, in this study the effect of building tilt is also included in the excitation term. It has been shown that by using the Lagrange equation, the generalized equation of motion for the fundamental sloshing mode can be written as (Tait 2008)

$$m^*\ddot{q}(t) + 2\zeta_{\mathrm{TSD}}\omega_{\mathrm{TSD}}m^*\dot{q}(t) + m^*\omega_{\mathrm{TSD}}^2 q(t) = \gamma^*\ddot{X}(t) \tag{6}$$

where $q(t)$ = generalized response coordinate of the fundamental sloshing mode; and the generalized mass, m^*, generalized damping ratio, ζ_{TSD}, angular natural frequency, ω_n, and excitation factor, γ^*, are given by (Tait 2008)

$$m^* = \frac{\frac{1}{2}\rho bL^2}{\pi\tanh\left(\frac{\pi h}{L}\right)} \tag{7}$$

$$\zeta_{\mathrm{TSD}} = C_l\sqrt{\frac{2}{\pi}\tanh\left(\frac{\pi h}{L}\right)}\Delta\Xi\frac{\sigma_q}{L} \tag{8}$$

$$\Delta = \frac{1}{3} + \frac{1}{\sinh^2\left(\frac{\pi h}{L}\right)} \tag{9}$$

$$\Xi = \sum_{j=1}^{ns}\left|\sin\left(\frac{\pi x_{sc}}{L}\right)\right|^3 \tag{10}$$

$$\omega_{\mathrm{TSD}} = \sqrt{\frac{\pi g}{L}\tanh\left(\frac{\pi h}{L}\right)} \tag{11}$$

$$\gamma^* = \frac{2\rho bL^2}{\pi^2} \tag{12}$$

where ρ = liquid density; g = gravitational acceleration; and σ_q = standard deviation of $q(t)$.

From Eq. (2), it seen that an effective acceleration, $\ddot{X}'$, can be written as

$$\ddot{X}' = \ddot{X} - g\theta - S_1\ddot{\theta} \tag{13}$$

where $\ddot{X}$ = lateral acceleration; $g\theta$ = acceleration produced by the component of gravity acting on the tank because of tilt; and the final term, $S_1\ddot{\theta}$, is due to the rotational acceleration of the tank, where for the first sloshing mode (Faltinsen et al. 2000)

$$S_1 = \frac{2L}{\pi}\tanh\left(\frac{\pi h}{2\mathrm{L}}\right) \tag{14}$$

The lateral and tilt components of the structural mode shape are defined as ϕ_X and ϕ_θ, respectively, and the generalized coordinate

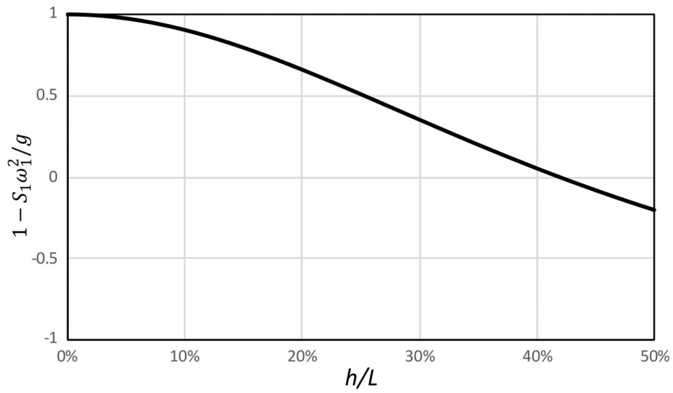

Fig. 3. Normalized plot showing relative variation of α terms.

of the structural mode of vibration is defined as $r(t)$. Since $r(t) \approx -\ddot{r}(t)/\omega_s^2$, the effective acceleration, $\ddot{X}'$ can be expressed as

$$\ddot{X}' = \phi_X \ddot{r}(t) + \frac{g\phi_\theta}{\omega_s^2}\ddot{r}(t) - S_1\phi_\theta \ddot{r}(t) \tag{15}$$

If $\alpha = [(g/\omega_s^2) - S_1](\phi_\theta/\phi_X)$, and $\ddot{X} = \phi_X \ddot{r}(t)$, then it is possible to write

$$\ddot{X}' = (1+\alpha)\ddot{X} \tag{16}$$

Since both g/ω_s^2 and S_1 are positive terms, increasing S_1 will decrease α. Fig. 3 shows the variation of the α terms for various depth ratios, h/L, and using the approximation $\omega_s \approx \omega_{\mathrm{TSD}}$. At low h/L, the term g/ω_s^2 dominates; however, when $(h/L) \approx 0.4$, the two terms nearly cancel each other. When $(h/L) > 0.4$, the term S_1 becomes larger, and therefore α becomes negative. However, most TSDs have depth ratios less than 0.25, so this will occur very rarely in practice, and tilt will therefore increase the TSD response and performance.

The mode shapes are eigenvectors and can therefore be scaled for convenience. Herein, the lateral component of the structural mode shape will be normalized to unity at the position of the tank, that is, $\phi_X = 1$ to simplify calculations; therefore, $\ddot{X} = \ddot{r}(t)$.

As before, the TSD is coupled to a structure with a generalized mass, damping constant, and stiffness of M, C, and K, respectively. The coupled equations of motion of the structure–TSD system with tilt are therefore

$$\begin{bmatrix} M+m_w & \gamma^* \\ (1+\alpha)\gamma^* & m^* \end{bmatrix}\begin{Bmatrix} \ddot{X} \\ \ddot{q} \end{Bmatrix} + \begin{bmatrix} C & 0 \\ 0 & 2\zeta_{\mathrm{TLD}}\omega_{\mathrm{TLD}} m^* \end{bmatrix}\begin{Bmatrix} \dot{X} \\ \dot{q} \end{Bmatrix} + \begin{bmatrix} K & 0 \\ 0 & \omega_s^2 m^* \end{bmatrix}\begin{Bmatrix} X \\ q \end{Bmatrix} = \begin{Bmatrix} F_{exc}(t) \\ 0 \end{Bmatrix} \tag{17}$$

where $F_{exc}(t)$ = generalized external wind excitation force. If there is no tilt ($\alpha = 0$), then this equation of motion collapses to be identical to that presented previously (Tait 2008). Following Tait's procedure, it is necessary to algebraically manipulate Eq. (17) to represent a linearized equivalent mechanical model as shown in Fig. 4. First, the substitution $x_r = \Gamma' q$ is made, where

$$\Gamma' = (1+\alpha)\Gamma \tag{18}$$

$$\Gamma = \gamma^*/m^* \tag{19}$$

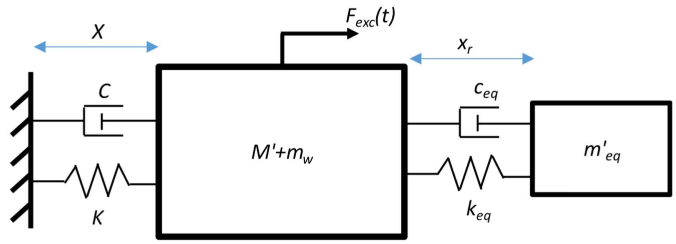

Fig. 4. Schematic of structure–TSD equivalent mechanical model.

Eq. (17) is now

$$\begin{bmatrix} M+m_w & \gamma^*\Gamma' \\ (1+\alpha)\gamma^* & \gamma^*\Gamma' \end{bmatrix}\begin{Bmatrix} \ddot{X} \\ \ddot{x}_r \end{Bmatrix} + \begin{bmatrix} C & 0 \\ 0 & 2\zeta_{\mathrm{TLD}}\omega_{\mathrm{TLD}} m^*\Gamma' \end{bmatrix}\begin{Bmatrix} \dot{X} \\ \dot{x}_r \end{Bmatrix} + \begin{bmatrix} K & 0 \\ 0 & \omega_s^2 m^*\Gamma' \end{bmatrix}\begin{Bmatrix} X \\ x_r \end{Bmatrix} = \begin{Bmatrix} F(t) \\ 0 \end{Bmatrix} \tag{20}$$

Then, the second equation is multiplied by Γ to yield

$$\begin{bmatrix} M'+m'_{eq} & m'_{eq} \\ m'_{eq} & m'_{eq} \end{bmatrix}\begin{Bmatrix} \ddot{X} \\ \ddot{x}_r \end{Bmatrix} + \begin{bmatrix} C & 0 \\ 0 & 2\zeta_{\mathrm{TLD}}\omega_{\mathrm{TLD}} m'_{eq} \end{bmatrix}\begin{Bmatrix} \dot{X} \\ \dot{x}_r \end{Bmatrix} + \begin{bmatrix} K & 0 \\ 0 & \omega_s^2 m'_{eq} \end{bmatrix}\begin{Bmatrix} X \\ x_r \end{Bmatrix} = \begin{Bmatrix} F(t) \\ 0 \end{Bmatrix} \tag{21}$$

where $M' = M + m_w - m'_{eq}$, and

$$m'_{eq} = (1+\alpha)m_{eq} \tag{22}$$

$$m_{eq} = \frac{\gamma^{*2}}{m^*} = \frac{8\rho b L^2}{\pi^3}\tanh\left(\frac{\pi h}{L}\right) \tag{23}$$

The equivalent TSD mass for a building with tilt given by Eq. (22) is equal to the equivalent mass of the TSD without considering building tilt, increased by a factor of $(1+\alpha)$. The parameter α is positive for tanks with $(h/L) < 0.4$ (see Fig. 3), which covers the range of practical TSD depth ratios. Considering tilt will therefore increase the equivalent mass and therefore efficacy of a TSD.

The structure–TSD mass ratio is given by $\mu = m'_{eq}/M'$. If the applied wind excitation is white noise with a power spectrum amplitude of S_0, the response spectra of the structure, $S_X(\omega)$, and equivalent TSD mechanical model $S_r(\omega)$ are

$$S_X(\omega) = S_0|H_X(\omega)|^2 \tag{24}$$

$$S_r(\omega) = S_0|H_r(\omega)|^2 \tag{25}$$

$$H_X(\omega) = \frac{-B_2\omega^2 + B_1 i\omega + B_0}{A_4\omega^4 - A_3 i\omega^3 - A_2\omega^2 + A_1 i\omega + A_0} \tag{26}$$

$$H_r(\omega) = \frac{B_2\omega^2}{A_4\omega^4 - A_3 i\omega^3 - A_2\omega^2 + A_1 i\omega + A_0} \tag{27}$$

where the constants are defined as (McNamara 1977)

$$A_0 = \omega_s^2 \omega_{TSD}^2$$
$$A_1 = 2\zeta_s \omega_s \omega_{TSD}^2 + 2\zeta_{TSD}\omega_{TSD}\omega_s^2$$
$$A_2 = \omega_s^2 + \omega_{TSD}^2(1+\mu) + 4\zeta_s\zeta_{TSD}\omega_s\omega_{TSD}$$
$$A_3 = 2\zeta_s\omega_s + 2\zeta_{TSD}\omega_{TSD}(1+\mu)$$
$$A_4 = 1 \quad (28)$$

$$B_0 = \omega_s^2 \omega_{TSD}^2$$
$$B_1 = 2\zeta_{TSD}\omega_{TSD}\omega_s^2$$
$$B_2 = \omega_s^2 \quad (29)$$

The spectral response of the wave height for the first sloshing mode is calculated through the relationship:

$$S_q(\omega) = \Gamma'^2 S_r(\omega) \quad (30)$$

where Γ' is previously defined. By integrating the spectra given by Eqs. (24) and (25), for white noise excitation the response variance of the structure and equivalent mechanical model are determined (McNamara 1977)

$$\sigma_s^2 = S_0\pi\left(\frac{\frac{B_0^2}{A_0}(A_2A_3 - A_1A_4) + A_3(B_1^2 - 2B_0B_2) + A_1B_2^2}{A_1(A_2A_3 - A_1A_4) - A_0A_3^2}\right) \quad (31)$$

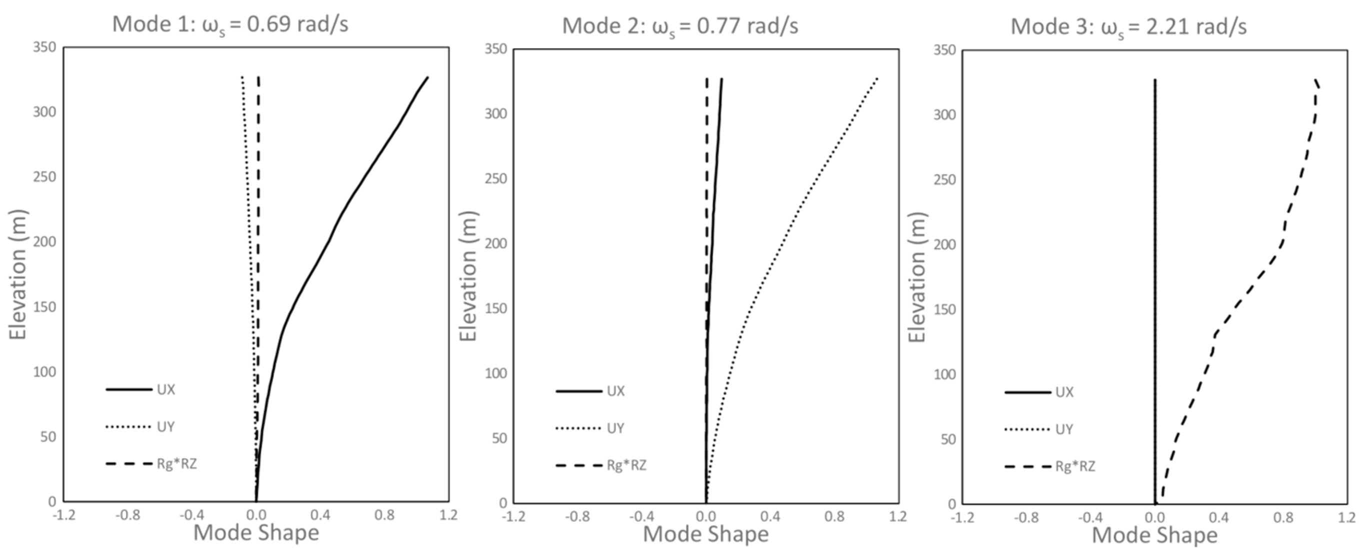

Fig. 5. Mode shapes of tower.

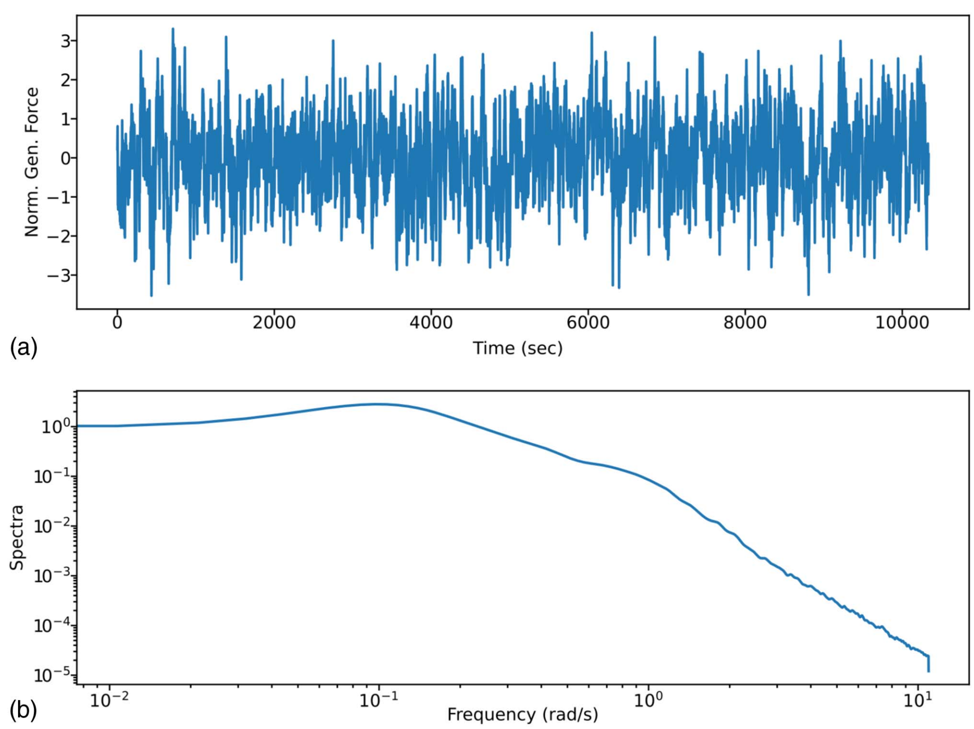

Fig. 6. Mode 1 generalized force: (a) time series; and (b) power spectral density function (10-year wind speed).

$$\sigma_r^2 = S_0\pi\left(\frac{A_1B_2^2}{A_1(A_2A_3 - A_1A_4) - A_0A_3^2}\right) \quad (32)$$

where σ_s and σ_r = standard deviations of the structure and equivalent mechanical system. The standard deviation of the first sloshing mode wave height is calculated using $\sigma_q = \Gamma'\sigma_r$. Since the TLD damping ratio is dependent upon σ_q, iteration is required to determine the solution. The mean peak hourly acceleration of the structure can then be predicted using Davenport's peak factor, $\hat{\ddot{X}} = PF \times \omega_s^2\sigma_s$, where (Davenport 1964)

$$PF = \sqrt{2\ln\left(3{,}600\frac{\omega_s}{2\pi}\right)} + \frac{0.577}{\sqrt{2\ln\left(3{,}600\frac{\omega_s}{2\pi}\right)}} \quad (33)$$

Note that peak wave heights are non-Gaussian, highly nonlinear, and substantially more challenging to predict using an equivalent mechanical model (Love and Tait 2019).

Case Study

Building

To demonstrate the implications of tilt on TSD performance, an anonymous real-world supertall building is considered as a case study. The reinforced concrete high-rise consists of a shear wall central core and three outriggers to engage the outer columns at elevations of approximately 120, 210, and 310 m. The tower is primarily residential with a height of approximately 330 m and typical floor dimensions of approximately 43 m × 27 m. The first three structural mode shapes are shown in Fig. 5 and have angular natural frequencies of 0.69, 0.77, and 2.21 rad/s, corresponding to X-sway, Y-sway, and torsional motion, respectively. The generalized mass of the first three modes is 17.2E6, 18.3E6, and 28.8E6 kg, respectively. The damping for all modes is assumed to be 1% of critical for service-level wind events analyzed herein, which is within the range recommended for tall concrete buildings (Biswas and Peronto 2020).

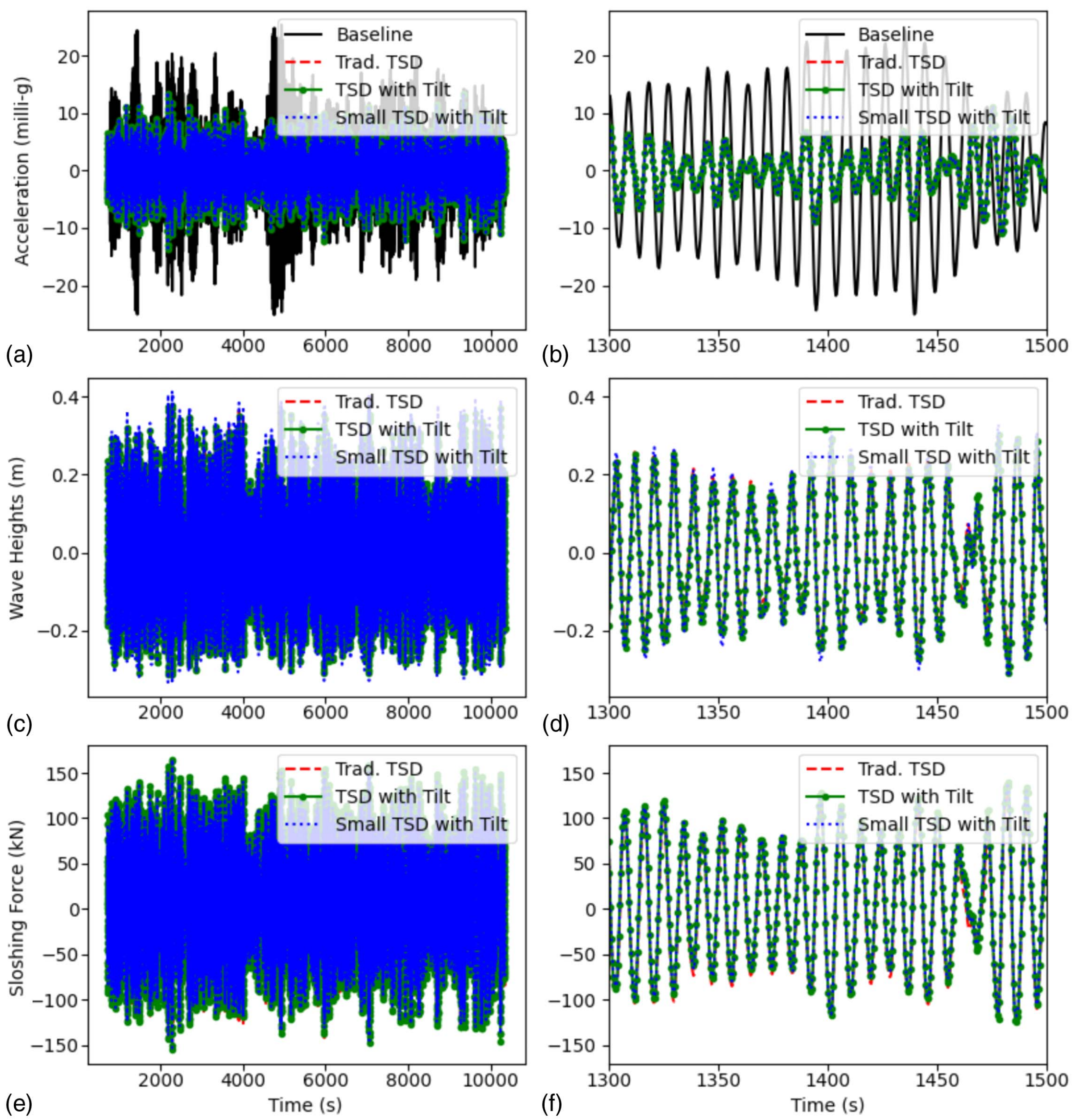

Fig. 7. Time series of system responses with various TSD configurations at 10-year wind speed: (a and b) tower acceleration; (c and d) TSD wave heights; and (e and f) sloshing forces.

The structure was tested in the wind tunnel using the high-frequency force balance technique, which has been described elsewhere (Irwin et al. 2013). The tower is particularly susceptible to excitation when winds are from 270° (west); therefore this wind direction will be the focus of this study. Note that in practice winds approaching from all wind directions are considered and integrated with a statical model of the wind climate to determine the response probabilistically. Moreover, only the response of Mode 1 (X direction) will be considered for simplicity. Fig. 6 shows the 10-year serviceability generalized force time series and power spectra for Mode 1 as determined from the wind tunnel test, which have been normalized to zero mean and unity variance. The wind speed associated with this loading is 39 m/s at gradient height (taken as 600 m). At this wind speed, the full-scale length of the excitation time series was approximately 2.9 h.

Tuned Sloshing Damper Systems

To demonstrate the effect that building tilt has on TSD performance, the tower Mode 1 response with and without including tilt in the simulations is investigated. The TSD is located at an elevation of 319 m, which is the penultimate floor, wherein ϕ_X and ϕ_θ are equal to 1.0 and 0.0054 rad, respectively. The TSD tank length is 22 m, with a width of 10 m and a quiescent water depth of 2.4 m. Screens are located at 25%, 50%, and 75% of the tank length, each with a screen loss coefficient of 5.0. With these TSD dimensions and mode shapes, $S_1 = 2.4$, and $\alpha = 0.10$.

The equivalent mass of the TSD is increased by a factor of 1.1 due to the inclusion of tower tilt [see Eq. (22)]. Therefore, the same level of TSD performance as the original tank can be maintained with a reduced TSD mass when considering tower tilt. To achieve this, the width of the tank can be decreased by dividing the original width by 1.1, yielding a new TSD tank width of 9.1 m. The simulations with tilt will be repeated with the 9.1 m tank to confirm it offers performance equivalent to the larger 10 m width tank when tilt is not considered.

The performance of each type of structure–TSD system is evaluated using the linearized equivalent mechanical model, as well as time-domain simulations of the structure–TSD system using the third-order multimodal model presented herein. Further information on the implementation details of the frequency-domain solution for the linearized model and the time-domain solution for the multimodal model is presented elsewhere for brevity (Love and Tait 2010; Tait 2008).

Results

Results of the time-domain simulations are presented in Fig. 7 for four cases: baseline (no TSD), traditional TSD without considering tower tilt (tank dimensions: 22 m × 10 m), a TSD with tower tilt (tank dimensions: 22 m × 10 m), and the smaller TSD tank with tower tilt (tank dimensions: 22 m × 9.1 m). The full time series as well as an enlarged 200-s segment of the tower acceleration, TSD wave heights, and TSD sloshing forces are shown in Fig. 7.

The equivalent mechanical model is solved in the frequency domain, and the resulting response tower acceleration and TSD wave height power spectra are shown in Figs. 8 and 9, respectively. The power spectra resulting from the nonlinear simulations are also shown for comparison, where both models are seen to agree.

The peak accelerations and wave height standard deviation results for all cases are summarized in Table 1. Standard deviations are used for the wave height comparisons, since it is challenging to estimate the peak wave heights using the equivalent mechanical model. The accelerations predicted by the two models are within 4% relative error. The inclusion of tilt increases the motion reduction performance of the TSD by a small, but measurable, amount. As a result, the tank width may be reduced from 10 to 9.1 m, and the same performance as the original tank without considering tilt was attained. The standard deviation of the wave heights increased when tilt was considered. The nonlinear simulations predicted a slightly larger wave response due to higher sloshing modes being included.

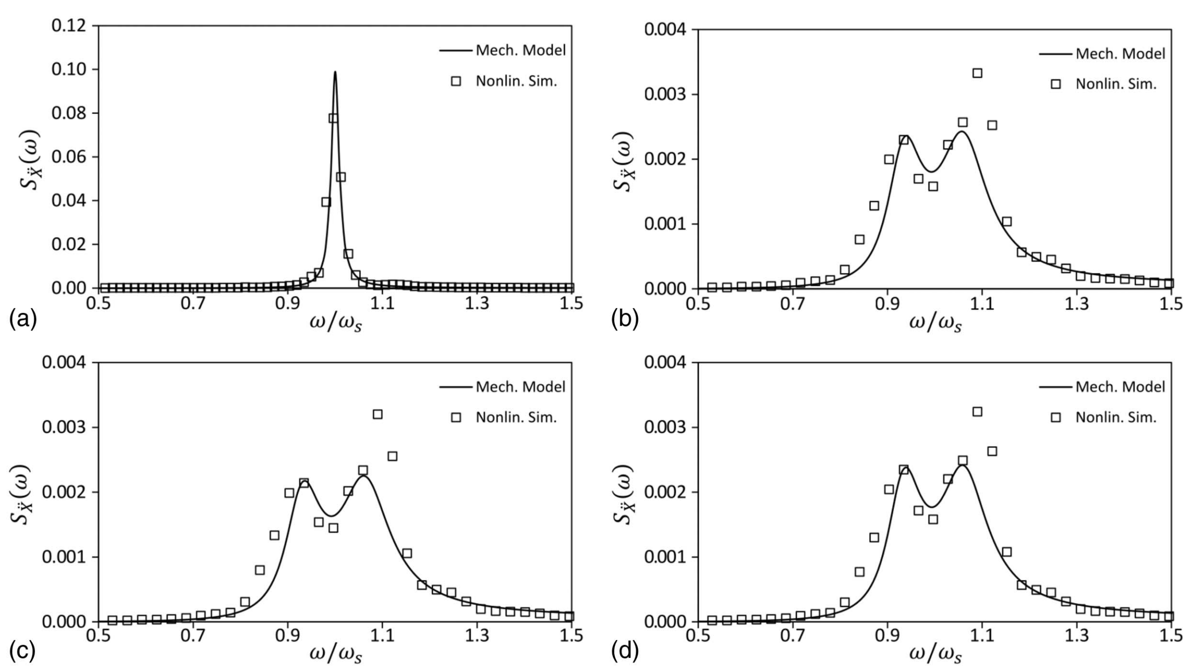

Fig. 8. Power spectra of tower acceleration predicted by mechanical model and nonlinear simulations: (a) baseline (no TSD); (b) traditional TSD (no tilt considered); (c) TSD considering tilt; and (d) smaller TSD tank considering tilt.

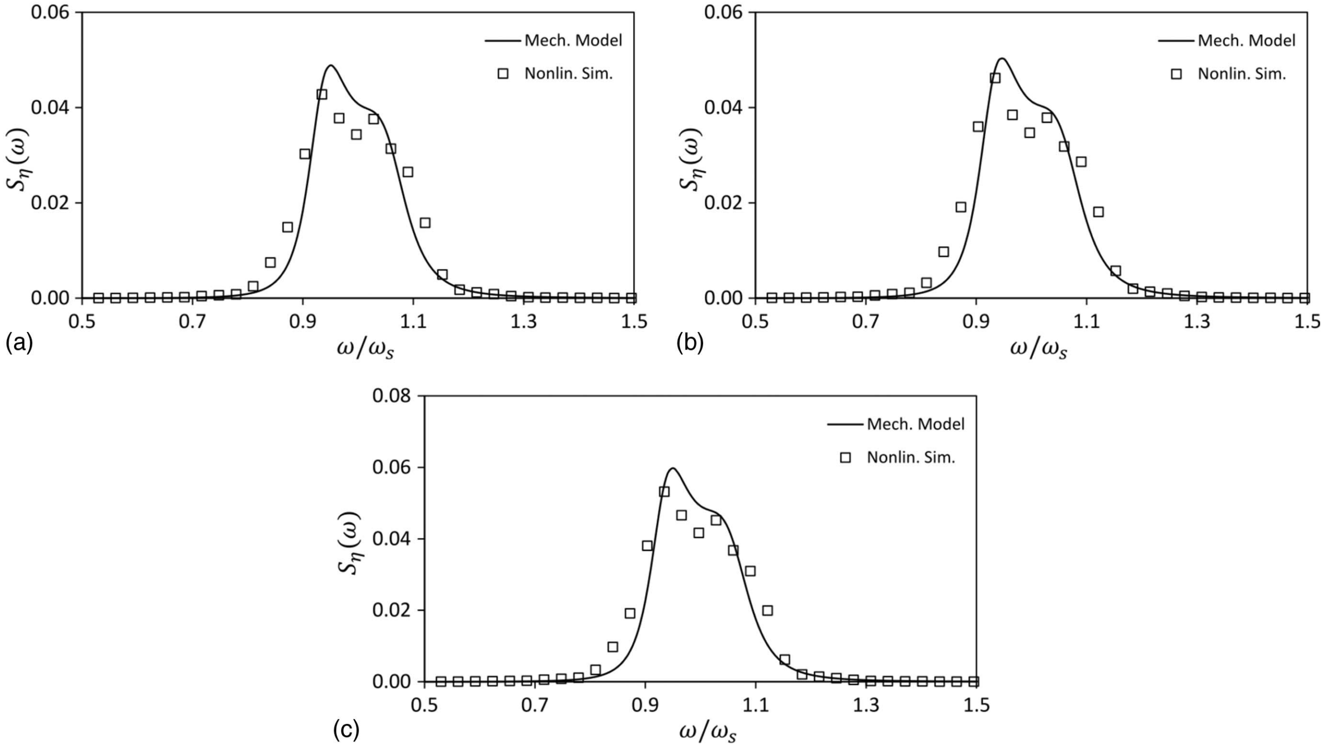

Fig. 9. Power spectra of TSD wave heights predicted by mechanical model and nonlinear simulations: (a) traditional TSD (no tilt considered); (b) TSD considering tilt; and (c) smaller TSD tank considering tilt.

Table 1. Summary of structure–TSD responses at 10-year wind speed

Variable	Prediction	Baseline	Without tilt	With tilt	Smaller tank with tilt
$\hat{\hat{X}}$ (milli-g)	Mech. model	24.6	11.9	11.7	11.9
	Nonlinear sim.	25.6	12.4	12.2	12.4
σ_q (m)	Mech. model	—	0.108	0.112	0.120
	Nonlinear sim.	—	0.116	0.121	0.129

The results have demonstrated that if floor tilt is included in the simulations, the tank width may be reduced by a factor of $(1+\alpha)$, resulting in considerable space savings of valuable real estate at the top of tall buildings. Since the per square meter value of real estate at the top of a luxury tall building is more than \$10,000 USD/m^2, the smaller TSD tank area savings may be valued at several hundred thousand dollars to the owner/developer.

700-Year Responses

The design wind loads were computed using the 700-year wind speed of 65 m/s for this Risk Category II building (ASCE 2017). Simulations are conducted at this wind speed to assess the response of the system and system loading at the ultimate wind event. Fig. 10 shows the results of the nonlinear simulations conducted at the 700-year wind speed, which are summarized in Table 2. At larger response amplitudes, the nonlinearities of the TSD response become more significant, and, as a result, the agreement between the mechanical model and nonlinear model worsens. Nevertheless, both models show that considering tilt yields accelerations that are approximately 2% lower than those that ignore tilt, although occupant comfort is not a design objective during the 700-year wind event. The wave heights and TSD tank base shears are both increased by approximately 4%–5% when tower tilt is considered. The TSD base shear with tilt is shifted slightly in the positive direction due to the building having a nonzero mean tilt according to Eq. (3), which produces a nonzero mean base shear. However, as discussed previously, this TSD force component is proportional to the tower displacement and will therefore not provide damping.

While a conservative motion reduction performance is calculated if tilt is neglected, neglecting tilt will lead to the underprediction of TSD loads and wave heights. Tower tilt should therefore be included in the structure–TSD model to more accurately reflect the actual performance of the system and to ensure that TSD design loads are not underestimated. When the TSD tank size is decreased because of the extra performance obtained by considering tower tilt, it is seen that the wave heights increase, but the tank base shear is similar to the original (larger tank without considering tilt) case, since a smaller mass of water is present.

Conclusions

This study has investigated how the tilt of tall buildings can affect the response of a coupled structure–TSD system. A nonlinear multimodal TSD sloshing model and a linearized equivalent mechanical model were presented that incorporate the dynamic tilt of a TSD due to building motion. The performance of a tall building equipped with a TSD was investigated, and the response of the structure–TSD system was considered if tilt was included or neglected in the analysis. The performance of a smaller tank considering tilt was also considered. The major findings of this study were the following:

- Tilt increases the effective lateral acceleration experienced by the sloshing fluid within the TSD tank due to a component of gravitational acceleration being engaged. An additional excitation

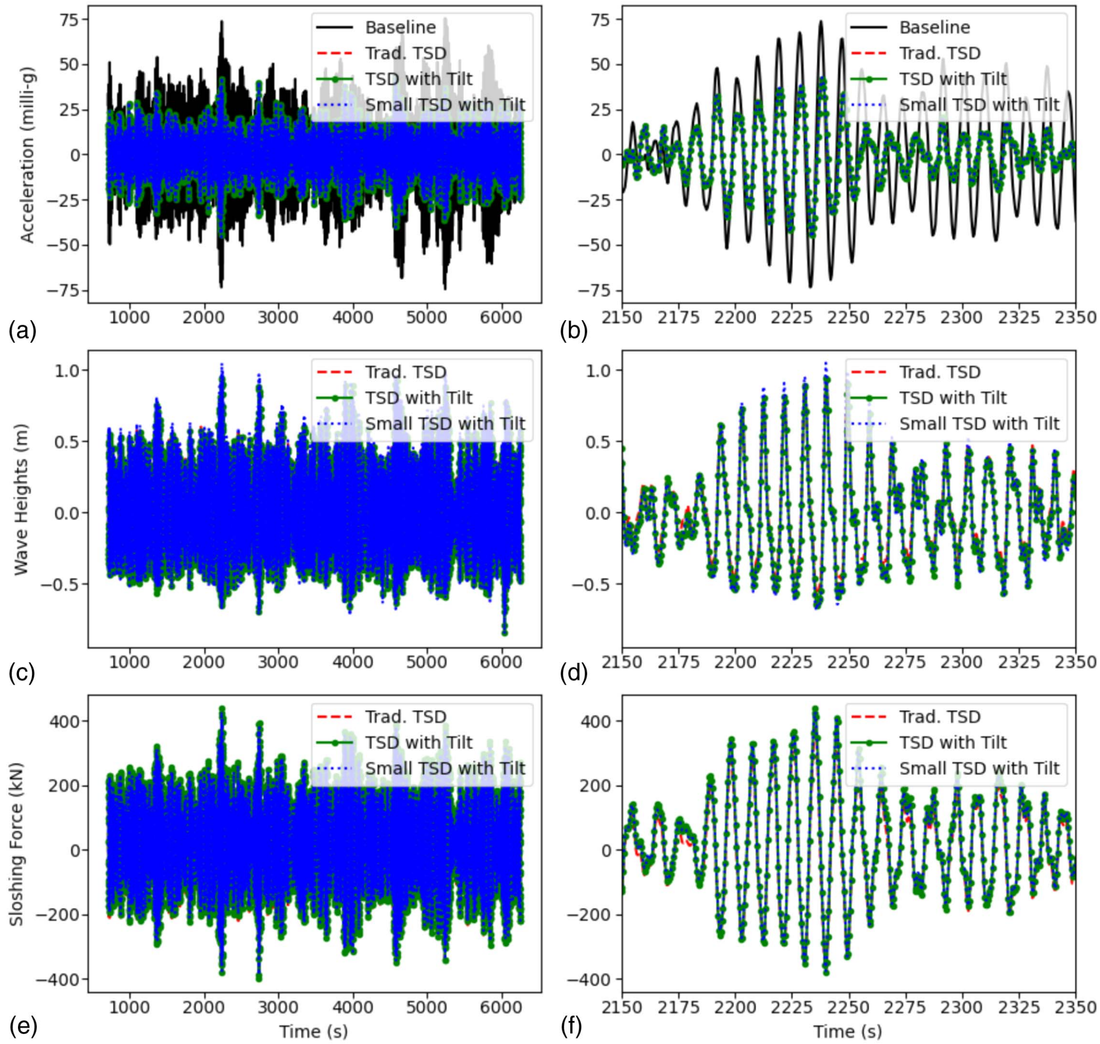

Fig. 10. Time series of system responses with various TSD configurations at 700-year wind speed: (a and b) tower acceleration; (c and d) TSD wave heights; and (e and f) sloshing forces.

Table 2. Summary of structure–TSD responses at 700-year wind speed

Variable	Prediction	Baseline	Without tilt	With tilt	Smaller tank with tilt
$\hat{\ddot{X}}$ (milli-g)	Mech. model	86.8	47.5	46.7	47.5
	Nonlinear sim.	82.5	41.2	40.4	41.2
σ_q (m)	Mech. model	—	0.242	0.252	0.268
	Nonlinear sim.	—	0.252	0.264	0.282
$\hat{F}_{sosh}$ (kN)	Nonlinear sim.	—	431	454	438

term related to the second derivative of tilt can reduce the tank excitation; however, for most TSD tank shapes this term will be relatively small.

- The TSD base shear forces applied to the structure have terms proportional to the tower tilt and second derivative of tilt in addition to the typical sloshing and lateral acceleration terms. The terms proportional to tilt are in phase with the tower displacement and acceleration and therefore do not dissipate energy.
- The equivalent mass of the TSD is increased due to tilt, which increases the motion reduction performance of the TSD system. For the case considered herein, the tilt increased the effective mass of the TSD by a factor of 1.1. The TSD tank width was reduced by a factor of 1.1, and the same performance reduction was attained with the consideration of tilt.
- Larger TSD response (wave heights and base shear forces) are produced when tilt is considered. It is therefore unconservative to neglect building tilt when establishing TSD design loads.

The inclusion of building tilt in the analysis of a TSD system will enable these devices to be designed more accurately and efficiently and will avoid the underprediction of design loads. It was demonstrated that smaller tank sizes can be employed for the same level of performance, which will increase the amount of saleable space near the top of tall buildings. A 10% reduction in tank plan area will yield material financial benefits to owners/developers building high-rise buildings in expensive urban centers.

Data Availability Statement

Some or all data, models, or code generated or used during the study are proprietary or confidential in nature and may only be provided with restrictions.

Author Contributions

J. S. Love: Conceptualization; Formal analysis; Writing – original draft. K. P. McNamara: Validation; Visualization; Writing – review and editing.

References

ASCE. 2017. *Minimum design loads and associated criteria for buildings and other structures*. ASCE 7-16. Reston, VA: ASCE.

Biswas, P., and J. Peronto. 2020. *Design and performance of tall buildings for wind*. Reston, VA: ASCE. https://doi.org/10.1061/9780784415658.

Caughey, T. K. 1963. "Equivalent linearization techniques." *J. Acoust. Soc. Am.* 35 (11): 1706–1711. https://doi.org/10.1121/1.1918794.

Davenport, A. G. 1964. "Note on the distribution of the largest value of a random function with application to gust loading." *Proc. Inst. Civ. Eng.* 28 (2): 187–196. https://doi.org/10.1680/iicep.1964.10112.

Faltinsen, O. M., O. F. Rognebakke, I. A. Lukovsky, and A. N. Timokha. 2000. "Multidimensional modal analysis of nonlinear sloshing in a rectangular tank with finite water depth." *J. Fluid Mech.* 407 (Mar): 201–234. https://doi.org/10.1017/S0022112099007569.

Faltinsen, O. M., and A. N. Timokha. 2001. "An adaptive multimodal approach to nonlinear sloshing in a rectangular tank." *J. Fluid Mech.* 432 (Apr): 167–200. https://doi.org/10.1017/S0022112000003311.

Faltinsen, O. M., and A. N. Timokha. 2009. *Sloshing*. New York: Cambridge University Press.

Griffis, L. 1993. "Serviceability limit states under wind load." *Eng. J.* 30 (1): 1–16. https://doi.org/10.62913/engj.v30i1.606.

Hu, W. H., Z. M. Xu, M. Y. Liu, D. H. Tang, W. Lu, Z. H. Li, J. Teng, X. H. Han, S. Said, and R. G. Rohrmann. 2020. "Estimation of the lateral dynamic displacement of high-rise buildings under wind load based on fusion of a remote sensing vibrometer and an inclinometer." *Remote Sens.* 12 (7): 1120. https://doi.org/10.3390/rs12071120.

Irwin, P., R. Denoon, and D. Scott. 2013. *Wind tunnel testing of high-rise buildings*. London: Routledge. https://doi.org/10.4324/9781315879529.

Irwin, P. A., L. A. Griffis, and W. F. Baker. 2019. *Serviceability design of tall buildings under wind load*. Redwood City, CA: Applied Technology Council.

Kareem, A., and W.-J. Sun. 1987. "Stochastic response of structures with fluid-containing appendages." *J. Sound Vib.* 119 (3): 389–408. https://doi.org/10.1016/0022-460X(87)90405-6.

Kwok, K. C. S., M. D. Burton, and A. K. Abdelrazaq. 2015. *Wind-induced motion of tall buildings*. Reston, VA: ASCE. https://doi.org/10.1061/9780784413852.

Lepelletier, T. G., and F. Raichlen. 1988. "Nonlinear oscillations in rectangular tanks." *J. Eng. Mech.* 114 (1): 1–23. https://doi.org/10.1061/(ASCE)0733-9399(1988)114:1(1).

Love, J. S., B. Morava, J. K. Robinson, and T. C. Haskett. 2021. "Tuned sloshing dampers in tall buildings: A practical performance-based design approach." *Pract. Period. Struct. Des. Constr.* 26 (3): 04021016. https://doi.org/10.1061/(ASCE)SC.1943-5576.0000582.

Love, J. S., and M. J. Tait. 2010. "Nonlinear simulation of a tuned liquid damper with damping screens using a modal expansion technique." *J. Fluids Struct.* 26 (7–8): 1058–1077. https://doi.org/10.1016/j.jfluidstructs.2010.07.004.

Love, J. S., and M. J. Tait. 2013. "Nonlinear multimodal model for TLD of irregular tank geometry and small fluid depth." *J. Fluids Struct.* 43 (Nov): 83–99. https://doi.org/10.1016/j.jfluidstructs.2013.09.009.

Love, J. S., and M. J. Tait. 2019. "Frequency domain prediction of peak nonlinear wave heights of structure-TLD systems." *Eng. Struct.* 194 (Sep): 1–10. https://doi.org/10.1016/j.engstruct.2019.05.033.

McNamara, K. P., B. N. Awad, M. J. Tait, and J. S. Love. 2021. "Incompressible smoothed particle hydrodynamics model of a rectangular tuned liquid damper containing screens." *J. Fluids Struct.* 103 (May): 103295. https://doi.org/10.1016/j.jfluidstructs.2021.103295.

McNamara, K. P., and M. J. Tait. 2022. "Modeling the response of structure–tuned liquid damper systems under large amplitude excitation using smoothed particle hydrodynamics." *J. Vib. Acoust.* 144 (1): 011008. https://doi.org/10.1115/1.4051266.

McNamara, R. J. 1977. "Tuned mass dampers for buildings." *J. Struct. Div.* 103 (9): 1785–1798. https://doi.org/10.1061/JSDEAG.0004721.

Pehlivan, H., Ö. Aydin, E. Gülal, and E. Bilgili. 2015. "Determining the behaviour of high-rise structures with geodetic hybrid sensors." *Geomatics Nat. Hazards Risk* 6 (8): 702–717. https://doi.org/10.1080/19475705.2013.854280.

Smith, B. S., and A. Coull. 1991. *Tall building structures: Analysis and design*. New York: Wiley.

Tait, M. J. 2008. "Modelling and preliminary design of a structure-TLD system." *Eng. Struct.* 30 (10): 2644–2655. https://doi.org/10.1016/j.engstruct.2008.02.017.

Tait, M. J., A. A. El Damatty, N. Isyumov, and M. R. Siddique. 2005. "Numerical flow models to simulate tuned liquid dampers (TLD) with slat screens." *J. Fluids Struct.* 20 (8): 1007–1023. https://doi.org/10.1016/j.jfluidstructs.2005.04.004.

Tamboli, A. R. 2014. *Tall and supertall buildings: Planning and design*. New York: McGraw-Hill.

Warnitchai, P., and T. Pinkaew. 1998. "Modelling of liquid sloshing in rectangular tanks with flow-dampening devices." *Eng. Struct.* 20 (7): 593–600. https://doi.org/10.1016/S0141-0296(97)00068-0.

Xia, Y., P. Zhang, Y. Ni, and H. Zhu. 2014. "Deformation monitoring of a super-tall structure using real-time strain data." *Eng. Struct.* 67 (May): 29–38. https://doi.org/10.1016/j.engstruct.2014.02.009.

Zhang, F. L., Y. P. Yang, H. B. Xiong, J. H. Yang, and Z. Yu. 2019. "Structural health monitoring of a 250-m super-tall building and operational modal analysis using the fast Bayesian FFT method." *Struct. Control Health Monit.* 26 (8): e2383. https://doi.org/10.1002/stc.2383.